Nanocomposite PECVD multiphase coatings for wear reduction under thermal load conditions

A. Nienhaus, G. Braeuer

Institute of Surface Technology, Technical University of Braunschweig

a.nienhaus@tu-braunschweig.de, guenter.braeuer@ist.fraunhofer.de

H. Paschke

Fraunhofer Institute for Surface Engineering and Thin Films IST

hanno.paschke@ist.fraunhofer.de

D. Stangier, W. Tillmann

Institute of Materials Engineering, TU Dortmund University

dominic.stangier@tu-dortmund.de, wolfgang.tillmann@tu-dortmund.de

M. Paulus, C. Sternemann

Fakultät Physik/DELTA, TU Dortmund University

michael.paulus@tu-dortmund.de, christian.sternemann@tu-dortmund.de

---

Abstract

With increasing demands for an enhanced service lifetime of tools, used in the hot forming and extrusion molding industry, new coating systems play an important role. Such applications demand a high thermal stability, high wear resistance, and low adhesion between the tool surface and hot metals (e.g. steel, aluminum, copper). Nanocomposite coatings consist of nm-size grains, embedded in an amorphous matrix. Due to their structure, they show a high hardness and wear resistance even under extreme conditions (high pressure, adhesive contact conditions, and high thermal loads). These multiphase coatings, generated from carbides, nitrides or borides of the transient metal titanium, provide the necessary properties for hot working applications. Currently, the binary and ternary phases TiN, TiC, TiB_2 or TiCN, TiBN are commonly used, yet limited concerning their thermal stability. The element spectrum Ti-B-N, Ti-C-N is expanded with silicon to synthesize interesting quaternary or quinary systems with typical nanocomposite

grain sizes of 3-7 nm. Recent in-situ phase analyses of the temperature-dependent phase transformation at 25 °C, 500 °C, and 750 °C revealed the possibility to optimize the mechanical properties by changing the structural composition in nanoscale dimensions. Tribological investigations under high-temperature conditions with a thermal load of 750 °C, and counterparts of Al_2O_3 spheres showed an improved wear resistance of the Si-containing systems compared to the non-Si systems. Assuming that Si and B containing films have a suitable low adhesion to many materials, further work should investigate the adhesive properties towards hot metals, e.g. aluminum and copper for extrusion molding applications.

1. Introduction

The demands for tool surfaces in hot forming applications such as aluminum and copper extrusion molding are constantly increasing due to high thermal loads and the chemical affinity between molten metal and the surface of the tool. Developing single-phase coatings, which provide a high hardness, low adhesion to molten metals, high toughness, thermal stability, oxidation resistance, and corrosive resistance is challenging [1]. Based on this spectrum of properties, multiphase hardcoatings with a nanocomposite structure ensure an enhanced overall performance and attracted much attention in recent years [1-10]. Nanocomposite coatings contain nanocrystalline (nc-) grains that are embedded in an amorphous (a-) matrix material (see *Fig. 1*) [2,3].

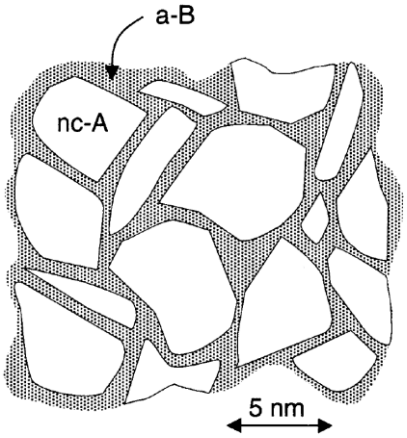

Figure 1: Schematic representation of a nanocomposite coating [2]

To obtain unique mechanical properties such as a high hardness and low Young`s modulus, the structure of these coatings is composed of 3–10 nm grains, which are separated by a 1–3 nm amorphous matrix [3–5]. For the coating system TiSiBCN, the most commonly detected crystalline phases are nc-TiN, nc-TiC, nc-TiCN, and nc-TiB_2 [1–4] while the amorphous matrix can contain a-C, a-BN, a-TiB_2, a-Si_3N_4, $TiSi_2$, etc. [4,5,7]. However, the phase evolution and tribological performance of TiSiBCN has not been understood yet.

2. Experimental details

2.1. Coating procedure

Ti-based hard coatings on Si wafers and hardened as well as tempered AISI H11 are deposited in a PECVD device (Ruebig GmbH & Co. KG). The substrates were cleaned for 15 min in an ultrasonic bath filled with isopropanol. Afterwards, the samples were exposed to a sequence of pretreatments such as 30 min sputtering for plasmacleaning and 30 min plasmanitriding with a low-pressure plasma. Plasmanitriding was carried out in an atmosphere with a low N_2 content (5 vol.-%) at p = 2.4 mbar, an applied bias voltage of U = -480 V, and a substrate temperature of T = 530 °C to increase the adhesion between the substrate and hard coating.

$TiCl_4$, BCl_3, CH_4, and $Si(CH_3)_4$ (tetramethylsilane, TMS) were used to synthesize TiBN, TiCN, TiBCN, and TiSiCBN. In addition, N_2 was used to form nitrogen-containing phases, while small quantities of Ar were utilized to support a stable glow discharge, and H_2 was added to reduce the chlorine content of $TiCl_4$ and BCl_3. The coatings were deposited at p = 2 mbar, U = -480..-580 V, and in a temperature range of T = 510–540 °C.

2.2. Coating characterization

The chemical composition was determined by means of electron probe microanalysis (EPMA). The hardness and Young's modulus were measured with a Nanoindenter G200 (Fa. Agilent). The nanocrystallites in the coating were characterized using a XRD at RT (ca. 25 °C) and in-situ with a thermal load of 500 °C and 750 °C, respectively. These XRD analyses were carried out at the beamline BL9 of the synchrotron light source DELTA (TU Dortmund University, Germany). The photon energy was set to 13 keV and a beam size with a width of 1.5 mm and height of 0.2 mm were used. Due to the small thickness of the deposited coatings, the angle of incidence was set to 1°. To avoid a free heat convection through air, a graphite dome was utilized to isolate the air from the surroundings as well as to ensure a constant temperature. A PILATUS 100K detector was used for the high-resolution XRD measurements with a step size of $\Delta 2\Theta = 0.1$ and an exposure time of 3 s. For better comparison, the diffractograms were converted into an energy level of CuKα (8.041 keV). For the tribological investigations, a pin-on-disc wear tester (Universal-Material-Tester 3, Fa. Bruckner) was used at elevated temperature. The specifications of the tribometer are summarized in *Table 1*.

Table 1: Parameters for high temperature wear

substrate	coating system	counterpart		wear tester parameters					
		material	radius	load	temperature	time	distance	diameter	speed
1.2343	TiBCN / TiSiBCN	Al_2O_3	5 mm	5 N	750 °C	900 s	3600 mm	20 mm	4 mm/s

3. Results and discussion

The chemical composition of TiBCN and TiSiBCN are listed in *Table 2*. The carbon content of the TiBCN coatings are low, whereas the content is high in the TiSiBCN coating. This is explained by the use of different CH_4 and TMS precursors, respectively. A high deposition rate of atoms from the TMS in the chamber, result in a Si + C diffraction of 49.4 at.-% and the amount of all other elements is significantly lower than in the TiBCN coating.

Table 2: Chemical composition [at.-%]

Coating	Ti	Si	B	C	N
TiBCN	49.2	-	15.8	3.4	31.6
TiSiBCN	28.1	17.2	1.4	32.2	21.1

The mechanical properties are summarized in *Table 3*. The coatings show a hardness of 11–34 GPa, but nanocomposites are known for hardness reaching > 40 GPa [3,10]. This is possibly the result of the high ratio of amorphous phases to nanocrystalline grains. The Young's modulus varies in a rather small range of 221–243 GPa, with the exception of TiCN coating with 342 GPa.

Table 3: Mechanical properties of the deposited coatings

Coating	Hardness [GPa]	Young's modulus [GPa]	Thickness [µm]
TiBN	16.0 ± 4.8	240.5 ± 46.0	0.8 ± 0.07
TiCN	26.5 ± 4.2	341.6 ± 38.5	2.8 ± 0.35
TiBCN - XRD	11.4 ± 1.2	233.5 ± 2.0	1.5 ± 0.22
TiBCN – wear tester	33.8 ± 1.1	242.7 ± 8.0	1.6 ± 0.08
TiSiBCN - XRD	20.5 ± 1.6	221.4 ± 11.9	4.8 ± 0.09
TiSiBCN – wear tester	17.9 ± 0.6	229.0 ± 5.2	2.7 ± 0.03

The diffractograms of the ternary TiBN system in dependency of the selected temperature levels are shown in *Fig. 2 a*. Only crystalline TiN phases can be identified at RT. With no characteristic reflex for TiB_2 being detected, B does not form a significant amount of crystalline phases. Thus it can be concluded that the B in the coating has to be amorphous, e.g. a-TiB_2 or a-BN [4,11]. At 500 °C, a thermally induced phase transformation was observed, which was also observed at 36° and 62° 2Θ in form of differently oriented TiN phases. At a temperature of 750 °C additionally leads to a strong oxidation of the Ti-phase, which forms TiO_2. The limited thermal stability that was determined is in agreement with He et al. [12] who annealed TiBN coatings for 4 h in an air atmosphere at 450 °C and 500 °C. Their XRD patterns showed both TiN and TiO_2 phases.

The ternary TiCN coating consists of TiC, TiN, and TiCN grains (see *Fig. 2 b.*). The characteristic reflexes of these phases overlap. In contrast to the TiBN coating, TiCN is thermally stable up to 500 °C with no observed phase transformation. At 750 °C, TiC, TiN, and TiCN phases are still detected. Additionally, a rather small amount of TiO_2 is discovered when compared to the TiBN coating. A phase transformation is detected as well, yet rather complex structures are formed, which need to be identified in additional investigations.

The quaternary TiBCN system behaves similar to the TiCN system, showing the characteristic reflexes for TiC, TiN, and TiCN (see *Fig. 2 c.*). With a B content of 15.8 at.-% and no TiB_2 reflexes detected, it is obvious that – as already reported for the TiBN coating – B is part of the amorphous matrix material. At 750 °C, TiBCN shows a quite similar phase transformation and oxidation behavior to the TiCN system.

The quinary TiSiBCN system is the only investigated system where up to a temperature of 750 °C neither phase transformations nor oxidations take place (see *Fig. 2 d.*). Again, characteristic reflexes for TiC, TiN, and TiCN are identified while no TiB_2 is detected. As mentioned before, a-TiB_2 and a-BN are presumed to occur in the phase composition, while the low B content (1.4 at.-%) indicates a minor fraction. A Si content of 14.2 at.-% and N content of 7.2 at.-% make the formation of a-Si_3N_4 very likely. Si_3N_4 is known as a diffusion barrier for oxygen in nanocomposite coatings, hindering the movement of oxygen along the grain boundaries [5,7,10]. For a more comprehensive understanding of the phase transformation investigations on an additional TiSiBCN coating, two TiSiBC coatings, and two TiSiCN coatings were carried out. For all these Si-containing coatings, neither phase transformations nor oxidations were detected. The TiSiBC coating does not contain any Si_3N_4 in the amorphous matrix because there is no N in the coating. Amorphous Si_3N_4 is often considered the main reason for the thermal

behavior of Si-containing coatings [5,7,10]. In-situ XRD measurements at 500 °C, 700 °C, and 900 °C were carried out by Mishra et al. with air surrounding the samples [13]. The results confirm the high thermal stability and oxidation resistance of TiSiBC. Therefore it can be concluded that other amorphous Si-containing phases than Si_3N_4 are formed, which enhance the thermal stability and oxidation resistance. It is further assumed that such phases could form in TiSiBCN coatings as well. The basic mechanisms behind the thermal behavior of Ti-based Si-containing coatings have to be further investigated.

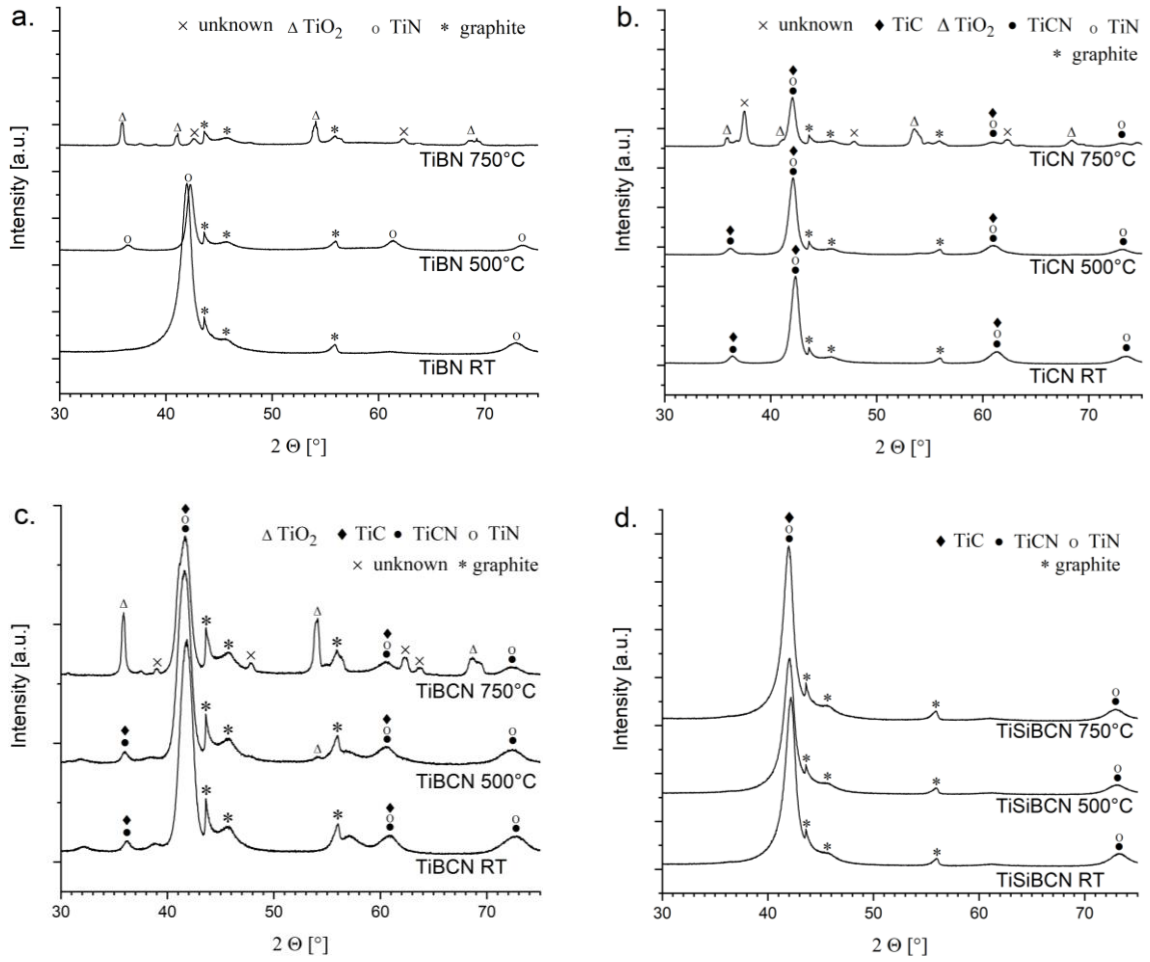

Figure 2: In-situ XRD-diffraction patterns at RT, 500 °C and 750 °C of a. TiBN, b. TiCN, c. TiBCN, and d. TiSiBCN

The wear resistance was investigated at 750 °C. TiBN was not thermally stable up to 500 °C and was therefore neglected. TiCN and TiBCN showed comparable results under thermal loads, but the chemical composition of TiBCN is comparable to that of the TiSiBCN system. The TiBCN coating, which was investigated by means of XRD showed a very low wear resistance with massive deformation of the coating and the

AISI H11 steel beneath. A harder (34 GPa) TiBCN coating with better adhesion properties to the substrate is found instead. The friction coefficient is $\mu = 0.28 \pm 0.07$ and hence much lower than the friction coefficient of $\mu = 0.39 \pm 0.08$ of the TiSiBCN coating. The friction coefficient of TiBCN constantly increases over time, beginning at an approximate average of $\mu = 0.2$ until $\mu = 0.4$ over 900 s (see *Fig. 3 a.*). In contrast, the friction coefficient of TiSiBCN constantly changes in the first 300 s and remains at approx. $\mu = 0.45$ for the following 600 s (see *Fig. 3 b.*). The already reported higher thermal stability and oxidation resistance of TiSiBCN and TiBCN does not necessarily lead to an increasing high-temperature wear resistance. The steadily increasing friction coefficient of TiBCN and the low thermal stability could prove to be fatal for tool surfaces in hot forming applications. However, for a short time duration of 900 s, the high hardness and toughness of the coating seem to prevail. Depositing TiSiBCN coatings with a comparable hardness and toughness could lead to even better results.

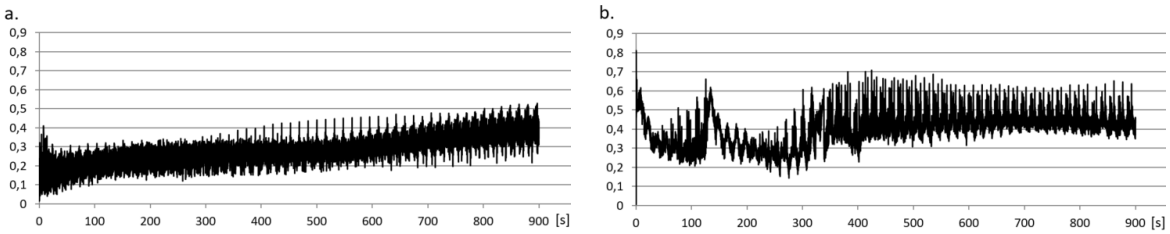

Figure 3: In-situ coefficient of friction of an a. TiBCN coating and a b. TiSiBCN coating over time

4. Conclusions

- The thermal stability and oxidation resistance of thin films were investigated by means of high-resolution XRD analyses at elevated temperatures. The Si-free coatings either formed TiO_2 or showed thermodynamically induced phase transformation from the as-deposited TiN, TiCN, TiC, etc. into more complex structures at 500–750 °C.
- Si-containing coatings were stable up to at least 750 °C. The two TiSiBC coatings, which were as well stable show that in addition to a-Si_3N_4, there exist more Si-containing phases, which increase the thermal stability and oxidation resistance.
- Future improvement of TiSiBCN coatings should create chemical compositions with less C and Si and more N and B, thus increasing the formation of nc-TiB_2 and nc-TiN grains and restraining the formation of a-C. These coatings would possibly achieve a so-called "superhardness" (> 40 GPa) and an even higher thermal stability (> 750 °C).

- Assuming that Si leads to a high temperature stability while B adds low chemical affinity towards molten metals, quinary TiSiBCN coatings should be tested for tool surfaces in extrusion molding processes. Yet, it is first necessary to improve coating properties such as the hardness and toughness.

Acknowledgement

The authors thank the DELTA machine group for providing the synchrotron radiation within Beamline 9.

Corresponding author

M. Sc. Alexander Nienhaus

Technical University of Braunschweig

Institute for Surface Technology

Eberhardstr. 12

D-44145 Dortmund

Telefon: 0231 / 844 - 3937

E-Mail: a.nienhaus@tu-braunschweig.de

Literature

[1] Mishra, S. K.; Mahato, P.; Mahato, B.; Pathak, L.C.: Thermal stability and effect of substrate temperature of TiSiBC hard nanocomposite coatings on microstructure, mechanical, thermal behavior deposited by magnetron sputtering, Applied Surface Science Vol. 266, p. 209-213, 2013.

[2] Mitterer, C.; Mayrhofer, P.H.; Beschliesser, M.; Losbichler, P.; Warbichler, P.; Hofer, F.; Gibson, P.N.; Gissler, W.; Hruby, H.; Musil, J.; Vlcek, J.: Microstructure and properties of nanocomposite Ti-B-N and Ti-B-C Coatings. Surface and coatings technology Vol. 120-121, p. 405-411, 1999.

[3] Veprek, S.; Niederhofer, A.; Moto, K.; Bolom, T.; Mannling, H.-D.; Nesladek, P.; Dollinger, G.; Bergmaier, A.: Composition, nanostructure and origin of the

ultrahardness in nc-TiN/a-Si_3N_4/a- and nc-$TiSi_2$ nanocomposites with HV=80 to >105 GPa, Surface & Coatings Technology Vol. 133-134, p. 152-159, 2000.

[4] Park, I.-W.; Mishra, B.; Kim, K.H.; Moore, J.J.: Multifunctional Ti-Si-B-C-N Tribological Coatings for Aerospace Applications. Materials Science Forum Vol. 539-542, p. 173-180, 2007.

[5] Thangavel, E.; Lee, S.; Nam, K.-S.; Kim, J.-K.; Kim, D.-G.; Synthesis and characterization of Ti-Si-C-N nanocomposite coatings prepared by filtered vacuum arc method. Applied Surface Science Vol. 265, p. 60-65, 2013.

[6] Lin, J.; Wei, R.; Bitsis, D.C.; Lee, M.L.: Development and evaluation of low friction TiSiCN nanocomposite coatings for piston ring applications. Surface & Coatings Technology Vol. 298, p. 121-131, 2016.

[7] Ma, S.L.; Ma, D.Y; Guo, Y.; Xu, B.; Wu, G.Z.; Xu, K.W., Chu, P.K.: Synthesis and characterization of super hard, self-lubricating Ti-Si-C-N nanocomposite coatings. Acta Materialia Vol. 55, p. 6350-6355, 2007.

[8] Kiryukhantsev-Korneev, P.V.; Shtansky, D.V.; Petrzhik, M.I.; Levashov, E.A.; Mavrin, B.N.: Thermal stability and oxidation resistance of Ti-B-N, Ti-Cr-B-N, Ti-Si-B-N and Ti-Al-Si-B-N films, Surface & Coatings Technology Vol. 201, p. 6143-6147, 2007.

[9] Pilloud, D.; Pierson, J.F.; Marco de Lucas, M.C.; Cacaleiro, A.: Study of structural changes induced by air oxidation in Ti-Si-N hard coatings. Surface & Coatings Technology Vol. 202, p. 2413-2417, 2008.

[10] Prochazka, J.; Karvankova, P.; Veprek-Heijman, M.; Veprek, S.: Conditions required for achieving superhardness of >45 GPa in nc-TiN/a-Si_3N_4 nanocomposites. Materials Science & Engineering A Vol. 384, p. 102-116, 2004.

[11] Lu, Y.H.; Shen, Y.G.; Li, K.Y., Chen, H.: Effects of nitrogen content on nanostructure evolution, mechanical behaviors and thermal stability in Ti-B-N thin films. Surface & Coatings Technology Vol. 201, p. 1228-1235, 2006.

[12] He, Y.; Zhou, J.; Walstock, T.; Duszczyk, J.: Oxidation behavior of PACVD TiBN coating at elevated temperatures. Surface & Coatings Technology Vol. 204, p. 601-609, 2009.

[13] Mishra, S.K.; Mahato, P.; Mahato, P.; Pathak, L.C.: Thermal stability and effect of substrate temperature of TiSiBC hard nanocomposite coatings on microstructure, mechanical, thermal behavior deposited by magnetron sputtering. Applied Surface Science Vol. 266, p. 209-213, 2013.